Reactive conversion of polycrystalline SnO_2 into single-crystal nanofiber arrays at low oxygen partial pressure

Carmen M. Carney and Sheikh A. Akbar[a)]
Department of Materials Science and Engineering, The Ohio State University, Columbus, Ohio 43212

Ye Cai and Sehoon Yoo
School of Materials Science and Engineering, Georgia Institute of Technology, Atlanta, Georgia 30332

Kenneth H. Sandhage[b)]
School of Materials Science and Engineering, School of Chemistry and Biochemistry, Georgia Institute of Technology, Atlanta, Georgia 30332

(Received 8 February 2008; accepted 4 June 2008)

Single-crystal SnO_2 nanofibers have been formed from SnO_2 polycrystals via reaction at low oxygen partial pressures. Polycrystalline SnO_2 disks coated with Au nanoparticles were exposed to humid H_2/N_2 at 700 to 800 °C. Single-crystal SnO_2 nanofibers formed beneath Au nanoparticles, with the nanofiber length oriented parallel to the [100] crystallographic direction of SnO_2. Because this simple process does not require either a separate source of a Sn–O-bearing vapor species located upstream of the substrate or a temperature gradient, single-crystal nanofibers may be formed on large area SnO_2-bearing substrates.

I. INTRODUCTION

Stannic oxide (SnO_2) based compositions possess attractive electrical, optical, and chemical properties for a number of device applications (e.g., as electrodes in solar cells,[1] light emitting diodes,[2] flat panel displays,[3] or batteries[4]; as catalysts[5,6]; as sensors[6–8] for CO, fuel gas, NH_3, or H_2O detection). Significant activity is underway to synthesize tin oxide based nanorods, nanowires, nanobelts, or nanotubes with high aspect ratios and well-controlled crystallinity for enhanced performance in such devices.[9–14] A number of authors have used vapor phase processes, which are typically conducted by generating a vapor precursor that is transported via a carrier gas (such as Ar or N_2) to a substrate, whereupon a single-crystal tin oxide based nanostructure is formed by deposition and growth.[9–21] The localized and sustained growth of high aspect ratio nanostructures on the substrate is accomplished through the use of a temperature gradient, metal catalyst particles (such as gold) deposited on the substrate, or both.

The purpose of the present paper is to demonstrate a simple reactive process for inducing the growth of oriented single-crystal nanofibers on a SnO_2-based substrate at low oxygen partial pressures at or below 800 °C. Unlike previously reported methods of tin oxide nanofiber or nanobelt synthesis employing vapor deposition techniques, the substrate itself acts as the vapor source in the present work, so that the need for a separate upstream source of vapor is obviated. Moreover, a temperature gradient is not required to induce the localized formation of nanofibers. By avoiding the need to establish a carefully controlled temperature difference between an upstream vapor source and the downstream substrate to induce the formation of tin oxide nanofibers, the simple, modest-temperature reaction process of the present work provides an attractive means of forming single-crystal nanofibers on SnO_2-based or SnO_2-coated substrates of large area.

II. EXPERIMENTAL

Polycrystalline SnO_2-based disks were used as both the substrate and Sn–O gas source. A mixture of 95 wt% SnO_2 (powder of 99.9% purity with 0.3 μm average particle size, Cerac, Milwaukee, WI) and 5 wt% CoO (powder of 99.5% purity with 10 μm average particle size, Cerac) was prepared. Prior work has shown that the CoO is an effective solid-state sintering aid for the densification of SnO_2.[22] This powder mixture was placed along with isopropanol and milling media into a 6.5 cm diameter jar and then ball milled for 6 h. The powders were dried and compacted into 0.64 cm diameter disks under a uniaxial pressure of 880 MPa in a stainless steel die by single-end compaction. The compacted disks were then sintered in an ambient atmosphere at 1500 °C for

Address all correspondence to these authors.
[a)]e-mail: akbar.1@osu.edu
[b)]e-mail: ken.sandhage@mse.gatech.edu
DOI: 10.1557/JMR.2008.0321

24 h. This sintering schedule yielded dense specimens with exposed grains exhibiting faceted surfaces and possessing an average size of ~8 μm [Fig. 1(a)].

Prior to exposure to a low oxygen partial pressure heat treatment, the sintered SnO_2-based disks were coated with gold nanoparticles. A thin gold layer was applied to the tin oxide disk by sputtering from a gold target at a rate of about 0.5 nm/s for 50 s (Pelco Model 3 Sputter Coater, Ted Pella, Inc., Irvine, CA). Subsequent heating at 700 to 800 °C for 2 h resulted in rearrangement of the gold layer into discrete gold nanoparticles on the surfaces of the tin oxide grains [Fig. 1(b)]. The gold nanoparticle-bearing tin oxide substrates were heated to a temperature in the range of 700 to 800 °C in a controlled-atmosphere tube furnace, and then exposed to a H_2-bearing gas mixture flowing at 1 L/min for 1 to 3 h. Initial experiments, conducted with a flowing dry 5%H_2/95%N_2 gas mixture, resulted in the complete reduction of SnO_2 to yield large molten Sn droplets on the substrate surface. In subsequent experiments conducted with a flowing humid H_2/N_2-bearing gas mixture (to raise the effective oxygen partial pressure[23]), the formation of molten tin droplets was suppressed. The humidified stream was generated by passing a mixture of 5%H_2/95%N_2 through water at room temperature (23 ± 2 °C) upstream of the heated SnO_2-bearing substrates. An oxygen sensor (CG 1000, Ametec, Pittsburgh, PA) was used to measure the oxygen fugacity associated with this flowing humid gas mixture. The measured oxygen fugacities were 2.3×10^{-21} and 2.8×10^{-21} atm at 700 and 800 °C, respectively.

The microstructure and crystal structure of the nanofibers were characterized by scanning electron microscopy (SEM; Philips XL-30, FEI Co., Hillsboro, OR) and transmission electron microscopy (TEM; JEOL 4000EX, Peabody, MA). TEM samples were prepared by sonication of the fibers from the substrate in isopropanol. The fibers were then deposited on a carbon-coated copper grid. Selected-area electron diffraction (SAED) patterns were obtained to determine the crystallographic orientation of the fibers and the orientation relation between the oxide fiber and gold tip.

III. RESULTS AND DISCUSSION

A. Nanofiber orientation

Exposure of the gold nanoparticle-coated tin oxide substrates to the humid hydrogen-bearing gas at 700 to 800 °C resulted in the growth of 100 to 200 nm diameter fibers. An increase in the exposure time resulted in an increase in the average nanofiber length, as is evident by

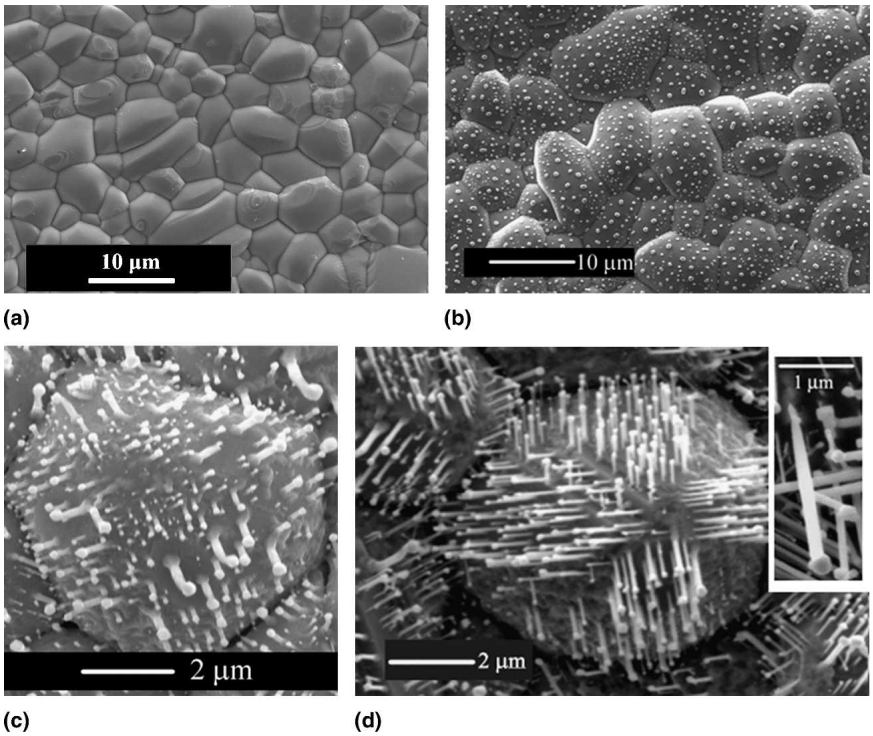

FIG. 1. SnO_2 nanofiber formation from microcrystalline SnO_2 via reaction with a H_2/N_2 gas mixture at 720 °C. Secondary electron (SE) images of the surfaces of polycrystalline SnO_2-bearing disks: (a) after sintering at 1500 °C for 24 h, and then (b) sputter deposition of gold followed by annealing in N_2(g) at 720 °C for 4 h (such heat treatment resulted in rearrangement of the gold layer into discrete gold nanoparticles). The scanning electron images in (c) and (d) reveal the SnO_2 nanofibers formed on the gold nanoparticle-bearing SnO_2 disks after exposure to a flowing humid 5% H_2/95% N_2 gas mixture at 720 °C for 1 and 2 h, respectively. The inset in (d) reveals a magnified view of several nanofibers with gold nanoparticles present at the nanofiber tips.

comparing Figs. 1(c) and 1(d). The nanofibers were oriented in particular directions relative to the faceted surfaces of the underlying tin oxide crystals. To evaluate the nanofiber crystal structure and orientation, as well as the nanofiber/gold interface, nanofibers were removed from the underlying tin oxide substrate via ultrasonication in distilled water. Transmission electron (TE) images of such an isolated nanofiber are shown in Fig. 2. Energy-dispersive x-ray analyses of the nanofiber (not shown) revealed the presence of only tin and oxygen. SAED analyses of the nanofiber [Fig. 2(b)] yielded patterns consistent with the rutile-type structure of SnO_2 (e.g., the

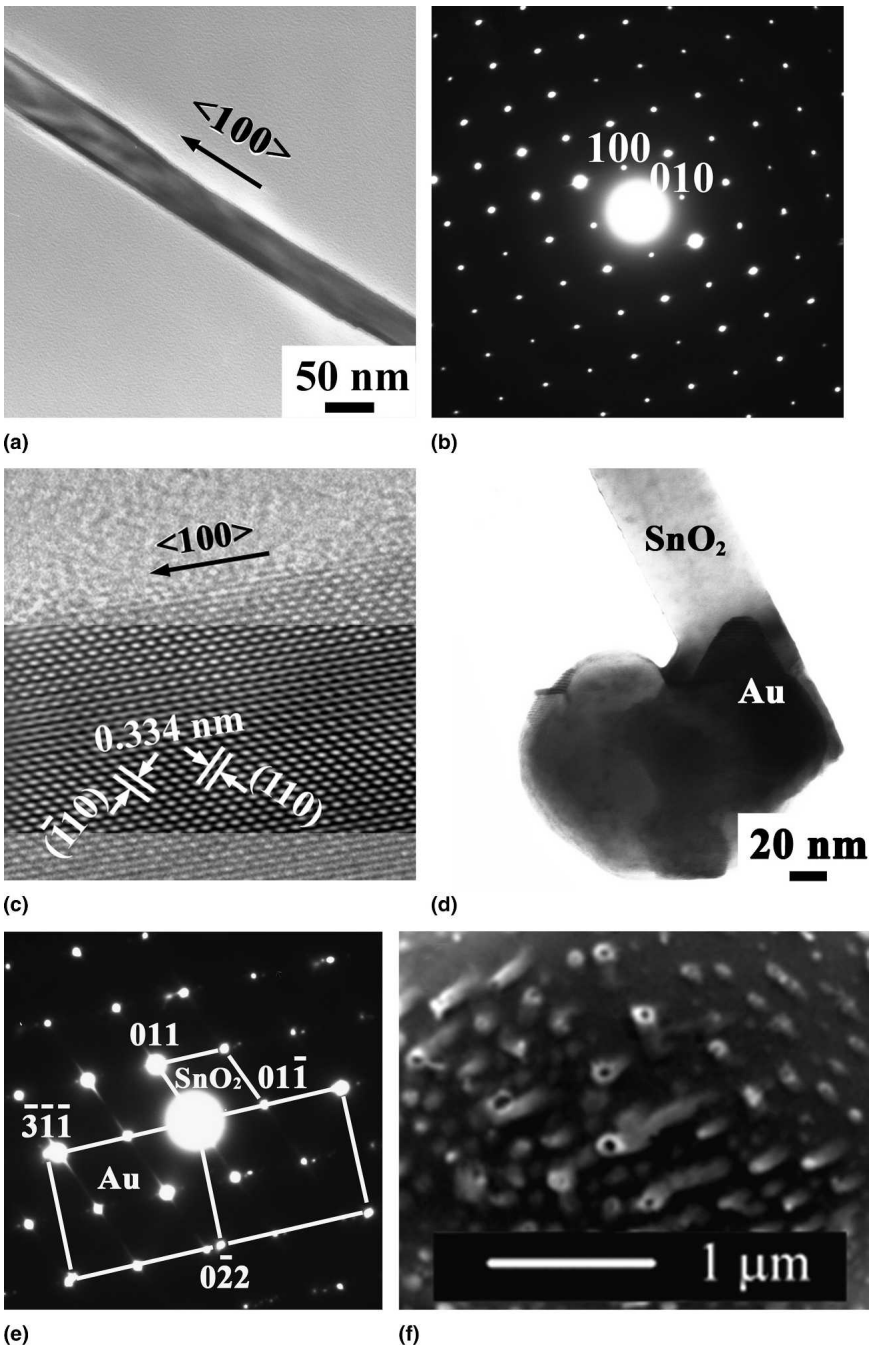

FIG. 2. Single-crystal SnO_2 nanofibers. (a) TE image of a single SnO_2 nanofiber. (b) SAED pattern of the nanofiber in (a). The orientation of the streaks in the electron diffraction spots was consistent with the ⟨100⟩ orientation of the long fiber axis. (c) High-resolution TE image obtained at the external edge of the nanofiber in (a). (d) TE image revealing a Au nanoparticle at the end of a SnO_2 nanofiber. (e) SAED pattern obtained at the interface between the Au tip and SnO_2 body. The Au and SnO_2 exhibited the following orientation relation: $[-233]_{Au}//[100]_{SnO_2}$ and $(331)_{Au}//(011)_{SnO_2}$. (f) Scanning electron image revealing the concave end surfaces of the SnO_2 nanofibers after selective dissolution of the Au nanoparticles.

measured "*a*" lattice parameter was 4.75 ± 0.04 Å, which was consistent with the reported value of 4.738 Å for SnO_2).[24] Multiple SAED analyses conducted along the length of a given nanofiber indicated that the fiber comprised a single crystal, with the fiber length oriented parallel to the [100] crystallographic direction of SnO_2. This fiber orientation was also confirmed with high-resolution TE images of the type shown in Fig. 2(c).

Gold nanoparticles originally present on the SnO_2 substrate were located at the top ends of the SnO_2 nanofibers, as revealed by a cross-sectional TE image in Fig. 2(d). SAED analysis obtained from Au/SnO_2 interfaces [Fig. 2(e)] indicated that the following predominant orientation relationship existed between the gold nanoparticle and tin oxide nanofiber: $[-233]_{Au}//[100]_{SnO_2}$ and $(331)_{Au}//(011)_{SnO_2}$. The top surfaces of the SnO_2 nanofibers were revealed by selective dissolution of the Au nanoparticles upon exposure to an aqueous 1.8 M KI solution for 1 min, followed by rinsing in distilled water. As observed in Fig. 2(f), the gold-bearing ends of the nanofibers appeared concave in shape; that is, the SnO_2 nanofibers formed cups that partially encapsulated the gold nanoparticles.

B. Influence of gold in nanofiber growth

The formation of single-crystal SnO_2 nanofibers only occurred on sintered SnO_2-based disk specimens containing the gold nanoparticles; that is, exposure of gold-free SnO_2-based specimens to the flowing humid H_2/N_2 gas mixture at 700 or 800 °C for up to 3 h did not result in nanofiber formation. To determine whether the gold nanoparticles were required as catalysts for sustained fiber growth, or just for the initiation of nanofiber formation, the gold nanoparticles were selectively dissolved (via immersion in the KI solution as mentioned previously) from the tips of nanofibers formed by exposure to the hydrogen-bearing gas mixture for 1 h at 720 °C. The gold-free fibers were then exposed to the hydrogen-bearing gas mixture for 3 more h at 720 °C. Secondary electron images of the same nanofibers after the 1 h exposure at 720 °C (prior to gold removal) and after the second 3 h/720 °C exposure are shown in Figs. 3(a) and 3(b), respectively. Comparison of the same fibers in both images revealed that little or no fiber growth occurred during the second 3 h/720 °C treatment, which indicated that the continued presence of the gold nanoparticles at the tips of the nanofibers was required for the sustained growth of the nanofibers.

Stannic oxide can be reduced to stannous oxide gas or tin gas via the following reactions:

$$SnO_2(s) \rightarrow SnO(g) + \tfrac{1}{2}\, O_2(g) \quad , \qquad (1)$$

$$SnO_2(s) \rightarrow Sn(g) + O_2(g) \quad . \qquad (2)$$

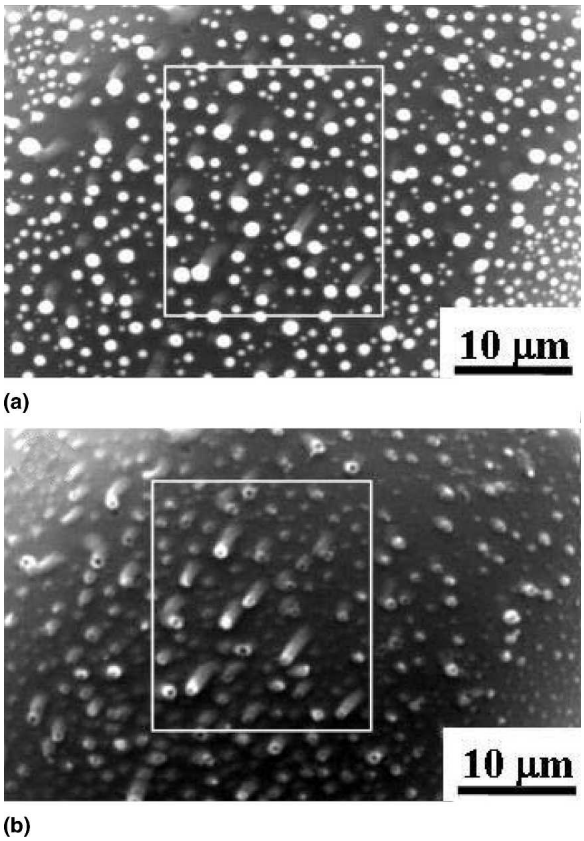

FIG. 3. Sustained SnO_2 nanofiber growth requires the presence of Au nanoparticles at the nanofiber tips. Scanning electron images of SnO_2 nanofibers grown (a) on a gold nanoparticle-bearing sample that was exposed to a humid 5%H_2/95%N_2 mixture at 720 °C for 1 h and (b) the same sample location after selective dissolution of the gold nanoparticles from the nanofiber tips and then re-exposure to the humid 5%H_2/95%N_2 mixture at 720 °C for 3 more h. The white boxes are provided as an aid to identify the same set of nanofibers in both images. Inspection of the same nanofibers in (a) and (b) indicated that no apparent growth of the Au-free nanofibers occurred during the second 3 h/720 °C H_2/N_2 treatment.

The equilibrium reaction constants for reactions (1) and (2) can be expressed as:

$$K_1 = f_{SnO_{(g)}}[f_{O_{2(g)}}]^{1/2}/a_{SnO_{2(s)}} \quad , \qquad (3a)$$

$$K_2 = f_{Sn(g)}f_{O_{2(g)}}/a_{SnO_{2(s)}} \quad , \qquad (4a)$$

where f_i and a_i refer to the fugacity and activity of species i, respectively. For SnO_2(s) present in its pure condensed reference state, and with the approximation that SnO(g), Sn(g), and O_2(g) behave as nearly ideal gases, these expressions become:

$$K_1 = p_{SnO(g)}[p_{O_{2(g)}}]^{1/2} \quad , \qquad (3b)$$

$$K_2 = p_{Sn(g)}p_{O_{2(g)}} \quad , \qquad (4b)$$

where p_i refers to the partial pressure of species i. The Gibbs free energies of formation of SnO_2(s), SnO(g), Sn(g) (obtained from Ref. 23) for reactions (1) and (2)

TABLE I. Gibbs free energies of formation of SnO_2(s), SnO(g), Sn(g) for reactions (1) and (2) and the calculated partial pressures [p_{SnO}(g) and p_{Sn}(g)].

Temperature (°C/K)	$\Delta G^o_f(SnO_2)$ (J/mol)	ΔG^o_f[SnO(g)] (J/mol)	$\Delta G^o_{rxn}(1)$ (J/mol)	K_1	p_{SnO}(g) (atm)
700/973	−378,336	−43,938	+334,398	1.12×10^{-18}	2.3×10^{-8}
800/1073	−357,693	−49,126	+308,567	9.53×10^{-16}	1.8×10^{-5}
Temperature (°C/K)	$\Delta G^o_f(SnO_2)$ (J/mol)	ΔG^o_f[Sn(g)] (J/mol)	$\Delta G^o_{rxn}(2)$ (J/mol)	K_2	p_{Sn}(g) [atm]
700/973	−378,336	+195,448	+573,784	1.58×10^{-31}	6.8×10^{-11}
800/1073	−357,693	+185,322	+543,015	3.68×10^{-27}	1.3×10^{-6}

Source: Ref. 23.

and the calculated partial pressures [p_{SnO}(g) and p_{Sn}(g)] are in Table I.

The oxygen partial pressures measured with a zirconia-based oxygen sensor resulting from the humid H_2/N_2 gas mixture were 2.3×10^{-21} atm at 700 °C and 2.8×10^{-21} atm at 800 °C. Using these values along with the thermodynamic data shown above, the calculated partial pressures of SnO(g) generated from reaction (1) at 700 and 800 °C were 1 to 3 orders of magnitude higher than the calculated partial pressures of Sn(g) generated from reaction (2). These calculations indicate that SnO(g) should have been the dominant tin-bearing gas species under the conditions used in these experiments.

C. Growth mechanism

The sustained growth of SnO_2 nanofibers required the continuous mass transport of tin and oxygen from the SnO_2 substrate to the nanofiber growth front. The vapor phase transport of SnO(g) from the polycrystalline substrate to the single-crystal nanofiber tip provided a possible means of mass transport of tin and some oxygen. Additional oxygen would still be required for the conversion of the SnO(g) into SnO_2(s) at the Au/SnO_2 interface. This additional source of oxygen could have been provided via a gas transport process [e.g., O_2(g) generated via reaction (1) or H_2O(g) introduced into the furnace] and/or via solid-state diffusion of oxygen anions from the substrate through the SnO_2 lattice of the single-crystal nanofiber. SnO_2 is an n-type oxygen-deficient oxide through which oxygen anion transport occurs via a vacancy diffusion mechanism.[25–28] The temperature dependence of the diffusion coefficient for oxygen, D_O, in tin oxide single crystals from 700 to 1000 °C has been reported by Kamp et al.[28] to obey the following expression:

$$D_O = \exp\{-4 + 2)\exp\{-1.1 + 0.3\ \text{eV}/kT\}\ \text{cm}^2/\text{s} \quad . \tag{5}$$

(Note: the crystallographic orientation dependence of D_O through single-crystal SnO_2 was found to be insignificant.[28]) At 720 °C, the value of D_O obtained from Eq. (5) is 4.8×10^{-8} cm^2/s. A rough estimate of the effective distance of oxygen diffusion through single-crystal SnO_2 can be obtained from the product $(D_O t)^{1/2}$, which corresponds to 190 μm for 2 h at 720 °C. This value is much greater than the observed lengths of single-crystal SnO_2 nanofibers formed under these conditions [<2.5 μm, as seen in the inset in Fig. 1(d)]. Hence, additional oxygen required for the conversion of SnO(g) into SnO_2 at the nanofiber tip could have been provided by the solid-state diffusion of oxygen from the substrate through the SnO_2 nanofiber.

IV. CONCLUSIONS

In summary, single-crystal SnO_2 nanofibers were formed on the surfaces of gold nanoparticle-coated SnO_2-based disks via a simple hydrogen-induced reaction process at only 700 to 800 °C. The long dimension of the nanofibers was oriented parallel to the [100] crystallographic direction of SnO_2. The top end of each growing SnO_2 nanofiber contained a gold nanoparticle, with a distinct orientation relation detected at the Au/SnO_2 interface. The formation and sustained growth of the SnO_2 nanofibers required the continued presence of the Au nanoparticles at the top ends of the nanofibers. Solid-state and/or gas phase diffusion paths provided possible mechanisms of mass transport of tin and oxygen from the substrate to the ends of the nanofibers for sustained nanofiber growth. Unlike previous vapor–solid or vapor–liquid–solid processes for forming single-crystal SnO_2 nanofibers, this hydrogen-induced surface rearrangement process did not require a separate Sn–O vapor source located upstream of the substrate. A temperature gradient was also not needed to induce the local formation and growth of the nanofibers. Hence, this simple low-temperature process can be an attractive method for forming single-crystal SnO_2 nanofibers over large area tin oxide based or tin oxide coated substrates.

ACKNOWLEDGMENTS

This project was financially supported by the National Science Foundation through NSF-IGERT Grant No. 0221678 and by the Air Force Office of Scientific Research through Grant No. FA9550-05-1-0092.

REFERENCES

1. B. O'Regan and M. Gratzel: A low-cost, high-efficiency solar cell based on dye-sensitized colloidal TiO_2 films. *Nature* **353,** 737 (1991).
2. J. Cui, A. Wang, N.L. Edleman, J. Ni, P. Lee, N.R. Armstrong, and T.J. Marks: Indium tin oxide alternatives—High work function transparent conducting oxides as anodes for organic light-emitting diodes. *Adv. Mater.* **13,** 1476 (2001).
3. K. Nomura, H. Ohta, K. Ueda, T. Kamiya, M. Hirano, and H. Hosono: Thin-film transistor fabricated in single-crystalline transparent oxide semiconductor. *Science* **300,** 1269 (2003).
4. Y. Idota, T. Kubota, A. Matsufuji, Y. Maekawa, and T. Miyasaka: Tin-based amorphous oxide: A high-capacity lithium-ion-storage material. *Science* **276,** 1395 (1997).
5. C.P. Nicholas and T.J. Marks: Sulfated tin oxide nanoparticles as supports for molecule-based olefin polymerization catalysts. *Nano Lett.* **4,** 1557 (2004).
6. M. Batzill and U. Diebold: The surface and materials science of tin oxide. *Prog. Surf. Sci.* **79,** 47 (2005).
7. K.J. Albert, N.S. Lewis, C.L. Schauer, G.A. Sotzing, S.H. Stitzel, T.P. Vaid, and D.R. Walt: Cross-reactive chemical sensor arrays. *Chem. Rev.* **100,** 2595 (2000).
8. P.G. Harrison and M.J. Willett: The mechanism of operation of tin(iv) oxide carbon monoxide sensors. *Nature* **332,** 337 (1988).
9. E. Comini, V. Guidi, C. Malagu, G. Martinelli, Z. Pan, G. Sberveglieri, and Z.L. Wang: Electrical properties of tin dioxide two-dimensional nanostructures. *J. Phys. Chem. B* **108,** 1882 (2004).
10. X.H. Chen and M. Moskovits: Observing catalysis through the agency of the participating electrons: Surface-chemistry-induced current changes in a tin oxide nanowire decorated with silver. *Nano Lett.* **7,** 807 (2007).
11. M.S. Arnold, P. Avouris, Z.W. Pan, and Z.L. Wang: Field-effect transistors based on single semiconducting oxide nanobelts. *J. Phys. Chem. B* **107,** 659 (2003).
12. Q.H. Li, Y.J. Chen, Q. Wan, and T.H. Wang: Thin film transistors fabricated by in situ growth of SnO_2 nanobelts on Au/Pt electrodes. *Appl. Phys. Lett.* **85,** 1805 (2004).
13. Z. Liu, D. Zhang, S. Han, C. Li, T. Tang, W. Jin, X. Liu, B. Lei, and C. Zhou: Laser ablation synthesis and electron transport studies of tin oxide nanowires. *Adv. Mater.* **15,** 1754 (2003).
14. Y. Liu, J. Dong, and M. Liu: Well-aligned "nano-box-beams" of SnO_2. *Adv. Mater.* **16,** 353 (2004).
15. C-F. Wang, S-Y. Xie, S-C. Lin, X. Cheng, X-H. Zhang, R-B. Huang, and L-S. Zheng: Glow discharge growth of SnO_2 nano-needles from SnH_4. *Chem. Commun.* 1766 (2004).
16. J. Hu, Y. Bando, Q. Liu, and D. Golberg: Laser-ablation growth and optical properties of wide and long single-crystal SnO_2 ribbons. *Adv. Funct. Mater.* **13,** 493 (2003).
17. J.X. Wang, D.F. Liu, X.Q. Yan, H.J. Yuan, L.J. Ci, Z.P. Zhou, Y. Gao, L. Song, L.F. Liu, W.Y. Zhou, G. Wang, and S.S. Xie: Growth of SnO_2 nanowires with uniform branched structures. *Solid State Commun.* **130,** 89 (2004).
18. J.Q. Hu, Y. Bando, and D. Golberg: Self-catalyst growth and optical properties of novel SnO_2 fishbone-like nanoribbons. *Chem. Phys. Lett.* **372,** 758 (2003).
19. Z.R. Dai, Z.W. Pan, and Z.L. Wang: Novel nanostructures of functional oxides synthesized by thermal evaporation. *Adv. Funct. Mater.* **13,** 9 (2003).
20. P. Nguyen, H.T. Ng, J. Kong, A.M. Cassell, R. Quinn, J. Li, J. Han, M. McNeil, and M. Meyyappan: Epitaxial directional growth of indium-doped tin oxide nanowire arrays. *Nano Lett.* **3,** 925 (2003).
21. Q. Wan, M. Wei, D. Zhi, J.L. MacManus-Driscoll, and M.G. Blamire: Epitaxial growth of vertically aligned and branched single-crystalline tin-doped indium oxide nanowire arrays. *Adv. Mater.* **18,** 234 (2006).
22. J.A. Cerri, E.R. Leite, D. Gouvea, E. Longo, and J.A. Varela: Effect of cobalt(III) oxide and manganese(IV) oxide on sintering of tin(IV) oxide. *J. Am. Ceram. Soc.* **79,** 799 (1996).
23. I. Barin: *Thermochemical Data of Pure Substances* (VCH Verlagsgesellschaft, Weinheim, Germany, 1995).
24. W.H. Baur and A.A. Khan: Rutile-type compounds. IV. SiO_2, GeO_2 and a comparison with other rutile-type structures. *Acta Crystallogr., B* **27,** 2133 (1971).
25. J. Maier and W. Gopel: Investigations of the bulk defect chemistry of polycrystalline tin(IV) oxide. *J. Solid State Chem.* **72,** 293 (1988).
26. J. Mizusaki, H. Koinuma, K-I. Shimoyama, M. Kawasaki, and K. Fueki: High temperature gravimetric study on nonstoichiometry and oxygen adsorption of SnO_2. *J. Solid State Chem.* **88,** 443 (1990).
27. Y. Li-Zi, S. Zhi-Tong, and W. Chan-Zheng: A study on the nonstoichiometry of tin oxides by coulometric titration. *Solid State Ionics* **50,** 203 (1992).
28. B. Kamp, R. Merkle, R. Lauck, and J. Maier: Chemical diffusion of oxygen in tin dioxide: Effects of dopants and oxygen partial pressure. *J. Solid State Chem.* **178,** 3027 (2005).